Wireless acquisition for Resistivity Index in Centrifuge – WiRI: A comparative study of three Pc-RI methods

Quentin Danielczick[1] *Ata* Nepesov[2] *Laurent* Rochereau[2] *Sandrine* Lescoulie[2] *Victor* De Oliveira Fernandes [2] and *Benjamin* Nicot[2]

[1]SeaOwl Energy Service, on behalf of TOTAL S.A Editorial Department, 64000 Pau, France
[2]TOTAL S.A, CSTJF – Experimentation Interpretation Synthesis Department, 64000 Pau, France

Abstract. Technological improvements and innovations are made to offer solutions with superior efficiency in terms of cost, quality, speed or all of them. In the SCAL field, the conventional resistivity index measurement (the porous plate technique) is a cost-effective method that provides good quality results but is very time consuming. For this purpose, several methods were developed to reduce the time taken to acquire resistivity measurements. In 2017, we proposed the Ultra-Fast Capillary pressure and resistivity index measurements (UFPCRI) combining centrifugation, NMR imaging and resistivity profiling. Since 2021 the Wireless Resistivity Index (WiRI) method allows the acquisition of capillary pressure and resistivity index in a matter of days. This method is based on a new in-house system to acquire wirelessly resistivity indexes along a rock sample during a centrifugation. The determination of resistivity versus saturation curve and the n exponent of Archie's Law is done thanks to an optimization algorithm. In this paper we present the results obtained from multiple simulations and experiments for: WiRI, UFPCRI and Porous Plate to discuss the advantages and drawbacks of each method in terms of reliability and experimental duration. Six rock samples are studied. A comparison of the three methods regarding the Archie's n exponent, resistivity indexes and capillary pressure curves is performed.

1 Introduction

Choosing or advising the right measurement solution for the right objective is one of the most important tasks for the petrophysicist in charge of a formation evaluation study. For this purpose, many books [1], [2] are suited to learn and understand the advantages and drawbacks of multiple methods for each laboratory core analysis experiment. These works are solid foundations for conventional methods. The aim of this paper is to bring a focus, and an update regarding the recent developments in determining Capillary pressure (Pc) and Resistivity Indexes (RI) in laboratory.

Since 1942 and the publication of Archie's Law [3] many methods have been proposed to estimate its parameters, particularly the n exponent. Historically, the experimental duration of the reference technique, the Porous Plate (PP) was substantial and multiple experiments were built to tackle this specific problem. Some known methods are the Continuous injection [4], FRIM [5][6] or more recently methods based on Nuclear Magnetic Resonance (NMR) for ultrafast m & n Archie's exponent determination [7]. Since 2017, we proposed two new methods to participate in the improvement of Archie's exponents determination while keeping the determination of the Pc curve with UltraFast Capillary Pressure and Resistivity Index (UFPCRI) [8] and Wireless Resistivity Index (WiRI) [9].

Whether for the reference PP or for the UFPCRI and WiRI experiment, determining Archie's n exponent and Pc requires measurements of resistivity, water saturation (Sw), and a knowledge of the capillary pressure. However, the way to measure these properties and the way to process these measurements, are different for each method.

The PP technique consists in applying multiple pressure steps and homogeneous saturation profiles. For each step a triplet "Resistivity index – Saturation – Pressure" is acquired. With multiple steps, RI/Sw and Pc/Sw curves are populated, and n exponent determined with linear regression of the log-log RI/Sw curve.

The UFPCRI method is based on inducing a non-uniform saturation profile with a centrifuge (as proposed by Green *et al.* [10][11]), measuring local Sw profile with NMR, measuring multiple resistivities along the sample (1 resistivity each 5 mm of sample) and repeating the sequence with multiple centrifuge steps. For each step multiple points of Pc/Sw and RI/Sw are available, allowing to perform faster than PP the determination of n exponent and Pc curve.

The WiRI experiment follows the same principle as the UFPCRI method. It uses the non-uniformity of the saturation induced by centrifuge, but no NMR is used to measure local saturation along the sample. A mean saturation is recorded using the production volume at the outlet of the sample. A wireless Resistivity measurement system is embedded in the centrifuge and a resistivity profile (1 measurement every 5 mm) is acquired during

the rotation. Then, assuming the validity of Archie's law, resistivity profiles are inverted using an optimization process between Archie's law and measured mean saturation.

To investigate the impact of the differences between these three methods and allowing readers to choose the method that best fits their needs, this work is a comparative study of each experiment in 2 steps:

1) Investigation through simulation with Monte Carlo approach [12]. The three experiments are numerically compared in the same conditions, with 3 different synthetic datasets (representing 3 different rocks) in order to assess whether a method is more suitable for one type of sample or another. The impact of measurement uncertainties is also investigated to provide a clear view on which parameter has the most influence on our results.

2) Comparison of results on real cases to show the advantages and limits of each method.

2 Materials and methods

2.1 Procedure for simulations

The advantage of simulations is to be able to carry out a large number of synthetic experiments in a short time. In addition, it allows to evaluate different treatments in the same configuration and therefore to compare the differences inherent in the processes without experimental bias. Many simulators (as SCORES [13], DuMu^X [14] or CYDAR [15]) are available to design, interpret and simulate Special Core Analysis (SCAL) experiments. In this study Cydar© is used to generate synthetic data but Lenormand *et.al.* [16] have shown that all simulators have given same results (for average saturation simulation) considering PP and centrifuge experiment simulations.

In order to compare PP, UFPCRI and WiRI processing, 3 synthetic samples (S1 – S2 – S3) were created with the same properties:

- Length (L) 50 mm, Diameter (d) 38 mm
- Porosity (Phi) 20 %, Pore Volume (Vp) 11.341 cc

The only variations are made on permeability, capillary pressure curves and irreducible saturations (Swi). Pc curves presented in Fig. 1 are generated from the "log(S-beta)" function with threshold Smax option. Parameters are listed in Table 1. Parameters "P0 (magnitude), "Pt (Threshold)" and the "Log(S-beta)" function are defined in the Cydar-SCAL User Manual [17].

Table 1. Pc parameters used in Cydar

	Perm (mD)	Swi (frac)	Sw-max (frac)	P0 (mb)	Pt (mb)
S1	10	0.1	1.0	0.05	0.005
S2	100	0.2	1.0	0.5	0.05
S3	1000	0.3	1.0	1	0.5

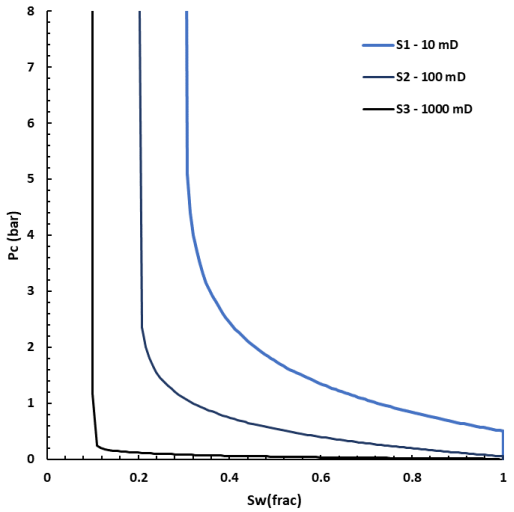

Fig. 1. Capillary pressure curves of synthetic samples S1, S2 and S3, generated with Cydar© and the set of parameters in Table 1

For each synthetic sample, Cydar is then used to generate datasets in Oil / Water drainage mode. Oil density and viscosity are 0.83 g/cc and 12 cP respectively. Water density and viscosity are set to 1 g/cc and 1cP.

- A Porous Plate experiment is simulated for each sample. It provides a production curve versus time. Production endpoints for each pressure steps are converted into resistivity using Archie's law with n = 2
- A centrifuge experiment is simulated for each sample. It provides multiple saturation profiles (with a 0.833 mm spacing between each saturation point) among time. They are converted into resistivity profiles using Archie's law with n = 2 and then "stacked" according to the UFPCRI and WiRI resistivity profiling resolution (with 5 mm spacing for each method)

Ultimately, 9 datasets are generated (3 experiments for each of the 3 samples).

In order to study the impact of uncertainties and differences between each process with a Monte Carlo approach, Matlab© is used to introduce different random normally distributed errors (through the "randn" function) [18] on each dataset. Each result presented was performed with a minimum of 100 000 simulation.

2.2 Rock samples and fluids for real cases experiments

For consistency between the simulated dataset and the experiments, we used samples with the same range of representative permeabilities, varying from 2100 mD (a Bentheimer outcrop sample), [80 – 400] mD (four reservoir sandstone rocks), and 11 mD (a Richemont outcrop sample).
For the UFPCRI and PCRI method the dimensions of the samples are d=38 mm and L=50 mm. For the WiRI experiment, due to the constraints of the system, plugs are d = 30 mm L = 45 mm. Fig. 2 shows the Klinkenberg corrected gas permeability (KgKl) versus Porosity (Phi) plot for samples used for WiRI (triangles), UFPCRI (rounds) and PCRI (squares). Twin samples have been used for every experiment except for the Richemont sample where PCRI and WiRI have been performed on the same sample d=30 mm L=45 mm (with a cleaning and drying sequence between each experiment).

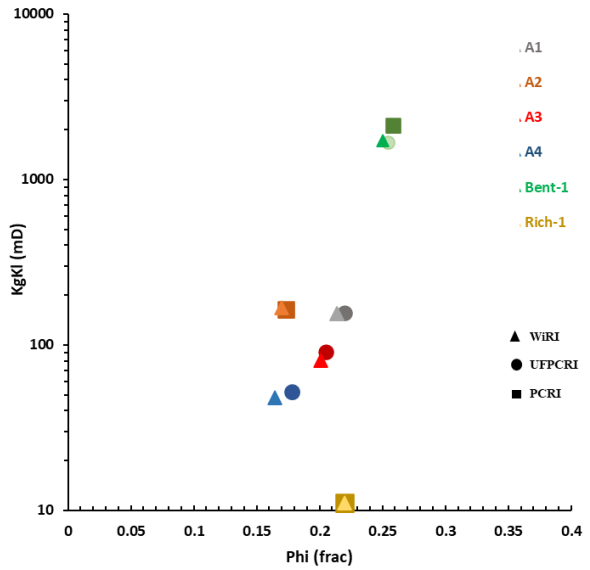

Fig. 2. Klinkenberg corrected gas permeability (logscale) versus porosity (Phi) of the studied samples

The fluids used for both experiments are summarised in Table. 2.

Table 2 : Fluid properties measured at 20°C

Samples	Heavy Fluid	Light Fluid
A1 – A4	Brine ρ = 1.01g/cc Viscosity = 1.075cP	Air ρ = 0.0012 g/cc Viscosity = 0.018 cP
Bent-1	Brine ρ = 1.052g/cc Viscosity = 1.45cP	Marcol52© ρ = 0.83g/cc Viscosity = 12.3 cP
Rich-1	Brine ρ = 1.052g/cc Viscosity = 1.45cP	Marcol52© ρ = 0.83g/cc Viscosity = 12.3 cP

2.3 Procedure for experiments

Both for the reservoir samples and for the outcrop samples the following routine core analysis (RCA) was performed before each experiment.

- Cleaning sequence of toluene and iso-propanol injections; nitrogen flushing; drying in the oven at 80°C
- Measuring dry mass and total volume
- Measuring helium porosity and gas permeability
- Saturating sample with synthetic brine (Sw=100%)
- Determining pore volume (Vp) from helium porosity and/or from weight difference between saturated and dry mass
- Determining fluid properties at 20 °C: brine density and resistivity (Rw), oil density

After the RCA, for the PP experiments:

- Mounting the core in an individual core holder with a porous plate saturated with the same brine
- Applying a confining stress of 50 bars
- Measuring initial resistivity Ro at Sw = 100%
- Applying a first pressure step and wait for production volume stabilization
- Applying multiple pressure steps with stabilization between each one
- Determine Pc/Sw, logRI/logSw curves, and n exponent with the end points of each pressure step

Tips to maximize PP data quality proposed by [19] have been followed. PP data is acquired when cessation of brine production and stabilization of resistivity is reached at each pressure step for 24 hours minimum. Interpretation is then performed on raw data.
For the UFPCRI and WiRI experiments the exact same sequences and equipment described in [8] and [9] are followed. For both methods, no confining pressure is needed.

3 Simulation Results

The aim of this study is to investigate the sensitivity of the 3 methods (PP, UFPCRI and WiRI) to various parameters. Sections 3.1 and 3.2 respectively show how a random error applied on produced volumes and on resistivities affects each method.

Section 3.3 presents the effect of classical errors (on volume and resistivity) on the results for different samples (Capillary pressure shape, permeability, saturation profiles) in this case the 9 datasets are analysed in parallel.

3.1 Effect of uncertainty on the produced volume Vprod

In this part, the results are shown for synthetic sample S2 but observations and interpretations are the same for each sample.
Here, a random absolute error is introduced on the "saturation part" of each method. For the PP and the WiRI

experiment, this error is introduced on the production volumes (representing an experimental error on the reading of volumes). The error is chosen "absolute" because whether in PP or in WiRI it is not dependent on the volume but only on the precision of the system. For UFPCRI the same error is applied directly on the "NMR" volumes generated. 100 000 simulations are performed for 8 normally distributed ranges of random error varying from 0 error to ±11 saturation units (s.u.). For each error range, we then obtain 100 000 results forming a distribution. The mean exponent n of the distribution is then plotted (Fig. 3) and the 5th and 95th percentiles are used as error bars. (A small shift on the x-axis between each method is applied for better reading. On the y-axis the shift is an observation of the simulation, not an artefact)

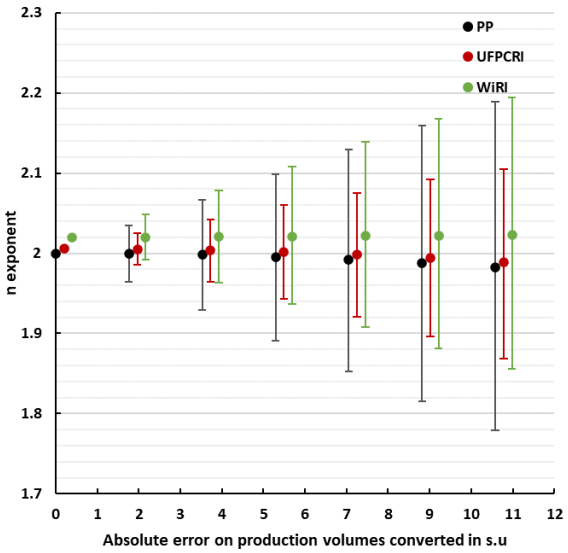

Fig. 3. Impact on each method of an increasing absolute error on production volumes

Observations:

For the PP, increasing the error on production volume leads to an obvious increase in range of error bars, but also to a far less obvious decrease of the mean n value. This is discussed in the interpretation section.

For UFPCRI: 3 observations could be done. First, even with 0 error a small systematic bias on the n exponent exists (n = 2.006 instead of 2). Second, increasing error leads to a drift towards lower mean n exponent. This second effect dominates the systematic bias. Third, the range of error bars increases with the error but is always lower than for PP and for WiRI

For WiRI: As for UFPCRI a systematic bias exists on the n exponent (even at 0 error n=2.019 instead of n=2). Error bars are also increasing with error but no further deviation on the mean is observed.

Interpretation:

First, the drift of the mean n with increasing error on produced volumes in PP and UFPCRI experiments is linked to the interpretation method. The two methods are based on a linear fit of RI versus Sw in log-log scale. Introducing an error on production volume will induce an "error bar" on the saturation. In linear scale the center of the error bar is given by the mean of the measurement, but as shown in Fig. 4 for illustration, an asymmetry appears on logscale. This asymmetry is even higher at lower saturation. In consequence, applying a linear fit on such a dataset leads, on average, to a lower n value than the searched value. Increasing the error on production volumes leads to increase the asymmetry and so, the probability to find an underestimated n value.

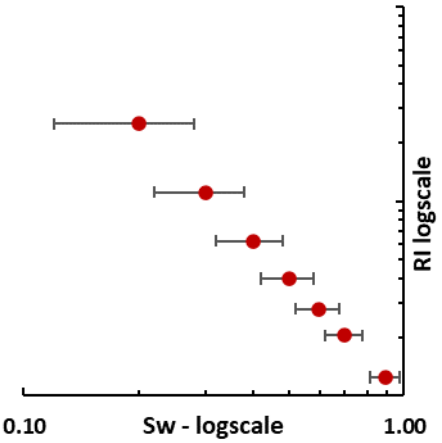

Fig. 4. Illustration of the asymmetry of the error bar on Sw in logscale

The process used in WiRI experiment to calculate the n exponent is based on the determination of the least squares between an estimator (containing the n exponent) and the measured produced volume. It explains why the same drift isn't observed.

Second, the systematic excess bias observed in UFPCRI and in WiRI arises because of non-uniformity of profiles and the resolution. For WiRI we showed in [9] that a 5 mm spacing induces a small systematic error (less than 1%) on the n exponent. Given that the saturation profiles induced in a centrifuge are known to generally have a convex shape (or flat at the very least), an insufficient resolution (for resistivity measurement) will average the profile upward and therefore increase the n exponent. These two methods are based on imaging (resistivity and saturation imaging for UFPCRI, and resistivity imaging only for WiRI). The steeper the profile, the less accurate the image. This effect is even stronger in WiRI than in UFPCRI. Indeed, while the UFPCRI interpretation is performed with a set of independent RI-Sw points, the WiRI inversion is performed on all the RI data at the same time. Therefore, one «bad average » point will impact all data.

3.2 Effect of uncertainty on Resistivity

Here, a random relative error varying from 0 to ±12 % is introduced on the resistivity part of each method. The error is normally distributed and considered relative because of the nature of the equipment's usually used (a precision that decreases with increasing measured values).
The results are also shown for synthetic sample S2 but the observations and interpretations are the same for S1 an S3.

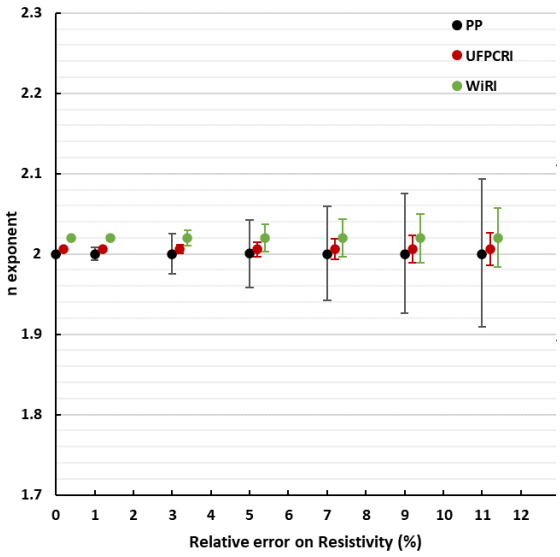

Fig. 5. Impact on each method of an increasing absolute error on resistivity

In Fig. 5, the error bar is the lowest for UFPCRI and the highest for PP method. The main explanation lies in the fact that the error applied in the resistivity is relative. In PP, one resistivity is measured for whole plug while for UFPCRI and WiRI resistivity is measured by sections of 5 mm. Consequently, for the same sample, measurement data in UFPCRI and WiRI are relatively small compared to PP, and therefore the errors too.

Comparing Fig. 4 and Fig. 5, the error on resistivity has a lower impact on the n exponent determination than the error on produced volume. The decrease in mean for UFPCRI and PP is not observed in this case. The following illustration (Fig. 6) allows to understand why an error in resistivity impact less the mean n value than an error in saturation. Even if asymmetry appears again, at low saturation the error bar is quasi-null in logscale and the method for determining n exponent forces the fit in 0, reducing the impact of error at high saturations.

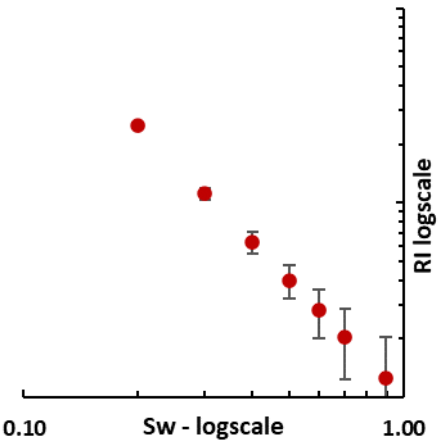

Fig. 6. Illustration of the impact of error in resistivity on the n exponent

3.3 Effect of the plug type (K,Pc) on the combined errors

In this part the investigation is presented for the 3 synthetic samples (S1 with K = 10 mD - S2 K = 100 mD - S3 K = 1000 mD and the associated Pc curves and Swi values presented in section 2.1) for the 3 methods. The 3 methods have been simulated (100 000 simulations) with a relative error in resistivity of ±5% and according to [1] an absolute error on produced volumes of ± 3 s.u. Results are the effect of the combined errors on the 3 methods for each sample "type". In Fig. 7, the lines represent the mean for each simulation and dotted lines the 5th percentile (P5) and 95th percentile (P95) confidence interval.

For the PP, the mean n of the 100 000 simulation is not dependent on the sample (the same mean n exponent). In contrast, the error bars (represented by the P5 and P95) decrease with increasing permeability. Indeed, applying the same pressure steps on a "higher permeability" sample (and lower Swi) would lead to higher produced volumes. Since the error on volumes, we introduced is absolute, this reduces the impact of error on saturations.

For UFPCRI the combination of errors approximatively has the same impact as the error on saturations only. The same small little bias due to resolution is observed and seems to grow for the higher permeability. The P5- P95 range on the n exponent shows to be the most reliable interval of confidence of all 3 methods.

For the WiRI: on the S1 and S2 (K = 10 mD and 100 mD), the combined errors on resistivity and on produced volumes lead to the same observation done in 3.1 (systematic excess bias on n exponent). The WiRI experiment shows a deviation of the average n calculated when error introduced, and the impact is more important for S3 with the higher permeability/lower Swi. It forces the mean n exponent away from the target. The confidence interval is tightening with permeability and the probability of finding a biased n is almost certain. The range P5-P95 is [2.08 - 2.13] instead of n = 2.

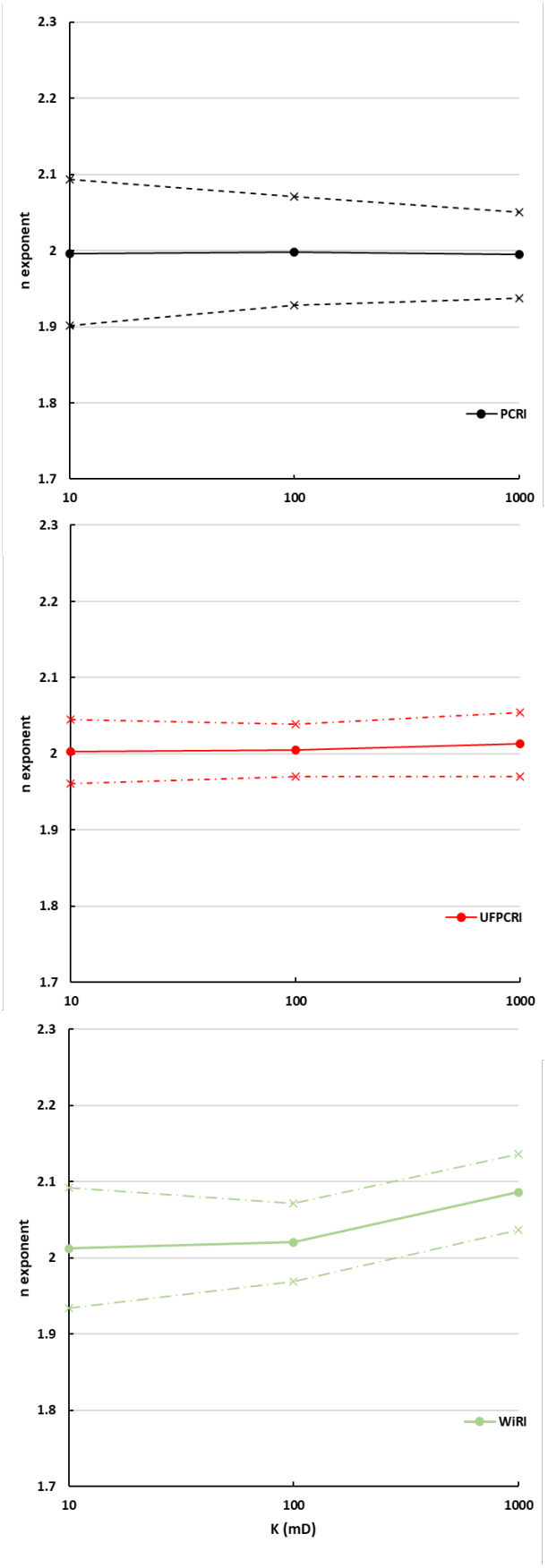

Fig. 7. Effect of the combined errors for each method and each sample

In 3.1 we saw that the WiRI inversion is performed on all the RI at the same time. Therefore, one «bad average » point will impact every single point in the optimization process. The resolution of WiRI measurements is limited by electrode spacing. When the permeability grows, it is more likely to find saturation profiles with stronger convexity. Therefore, the impact on WiRI inversion is higher at higher permeabilities.

4 Experimental results

Here we compare the experimental results obtained on real samples with various experimental methods (PP, UFPCRI and WiRI). For consistency with previous sections, we present the results obtained for high, middle and low permeability samples (Fig. 8 and Fig. 9).

Table 3: n exponent and Swi for Benth-1 – A1 – A4 – Rich-1 and the methods investigated for each sample

Samples	n exponent	Swi (frac)
Benth-1	PP: 1.83 UFPCRI: 1.74 WiRI: 1.78	PP: 0.10 UFPCRI: 0.12 WiRI: 0.08 (MICP): 0.09
Rich-1	PP: 1.80 WiRI: 1.72	PP: 0.35 WiRI: 0.36
A1	UFPCRI: 1.33 WiRI: 1.30	UFPCRI: 0.09 WiRI: 0.08 (MICP): 0.10
A4	UFCPRI: 1.45 WiRI: 1.29	UFPCRI: 0.11 WiRI: 0.9 (MICP): 0.15

For the sample Bentheimer-1 (top of Fig. 8): The Pc of PP and UFPCRI coincide, and MICP and WiRI also almost superimpose. The n exponents (Table. 3) are close, and the highest n is found for the PP method. This is in contradiction with the high permeability simulations (Fig. 7) predicting a higher n for the WiRI than for the two other methods. Other sources of uncertainty as handling, plug conditioning, measurement techniques and technologies have hidden, in that case, the bias on the n exponent. However, local saturation points and n exponent are both determined at the same time in the WiRI inversion. In 3.1 we observed that WiRI resolution present a systematic upward bias on the n exponent when determining least squares with a 5 mm resolution. In this specific case, measurements of local resistivities and produced volumes have led to determine an n exponent in the interval of PP and UFPCRI. Consequently, it seems logical to find WiRI saturations impacted downwards. Saturations determined by WiRI method are lower (-3 s.u. in average) than saturations determined by PP and UFPCRI at the same Pc.

For sample Richemont-1 (bottom of Fig. 8): Swi has not been reached for both experiments due to leaks, and handling issues. Difference between n (WiRI) and n (PP) is less than 0.1. For the part of the Pc curve investigated, Porous Plate and WiRI curves almost superimpose.

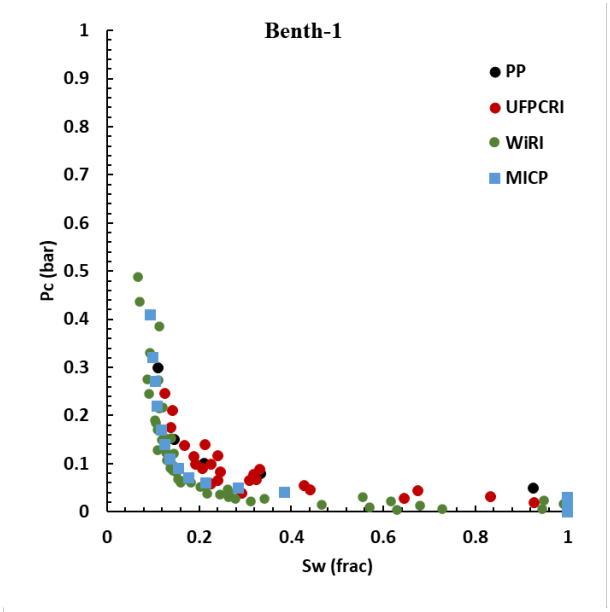

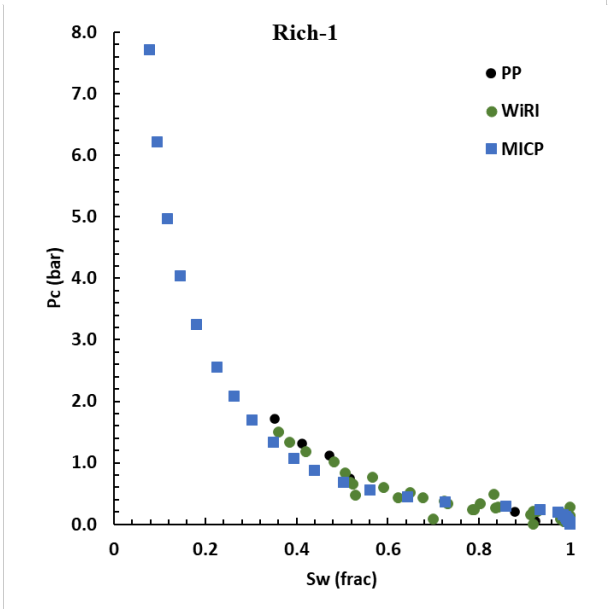

Fig. 8. Pc/Sw (Oil/Water Drainage) for: Benth-1 – K = 1700 mD and Rich-1 – K= 10 mD

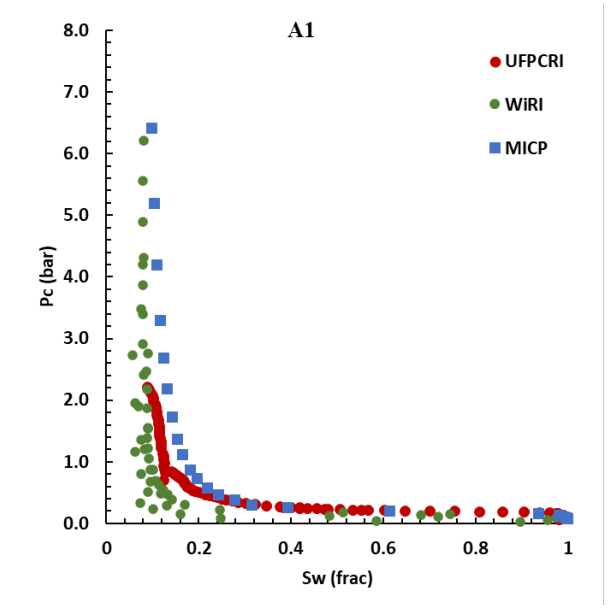

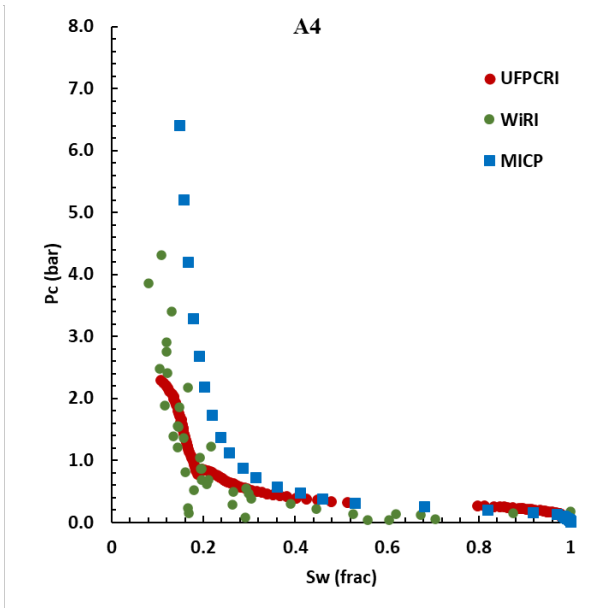

Fig. 9. Pc/Sw (Gas/Water Drainage) for: A1 - K = 150 mD and A4 - K = 50 mD

For samples A1 and A4 (Fig. 9): Pc curves obtained with each method show the same behaviour but deviations of saturation at the same pressure is shown (±4 s.u in average between WiRI and UFPCRI). Swi agrees with better accuracy (± 2 s.u maximum). No "overestimation" of the n exponent is provided by WiRI and last, MICP has a slightly higher Swi for both samples.

These 4 experiments also prove that uncertainty on measurements, noise, equipment, and operators are the major factors influencing the results of PP, UFPCRI and WiRI. Quality of the results is also affected by the homogeneity of the samples and heterogeneity may well dominate all measurement errors. Effect of heterogeneity is discussed in section 5. However, each experiment showed consistency in terms of n exponents and deviations on saturations at same pressure steps are less than 5 s.u in average despite the sources of measurement uncertainties.

5 Discussion: limitations of WiRI

This part tackles the limitations of the WiRI experiments through 2 main examples on real cases:

- The first limitation is the heterogeneity of a sample. As stated in [9] WiRI is based on the inversion of Archie's law along a sample and implies the homogeneity. An example of WiRI results on non-homogenous sample is shown Table. 4 and Fig. 10
- The second limitation is linked to a "non-Archie behaviour" of the resistivity-saturation data. Because Archie is an assumption of WiRI, a non-Archie behaviour cannot be spotted. This is shown in Fig. 12

Effect of heterogeneity:

Table 4. n exponent and Swi for sample A3 obtained with UFPCRI and WiRI

Sample	n exponent	Swi (frac)
A3	UFPCRI: 1.08 WiRI: 1.74	UFPCRI: 0.12 WiRI: 0.17 (MICP): 0.1

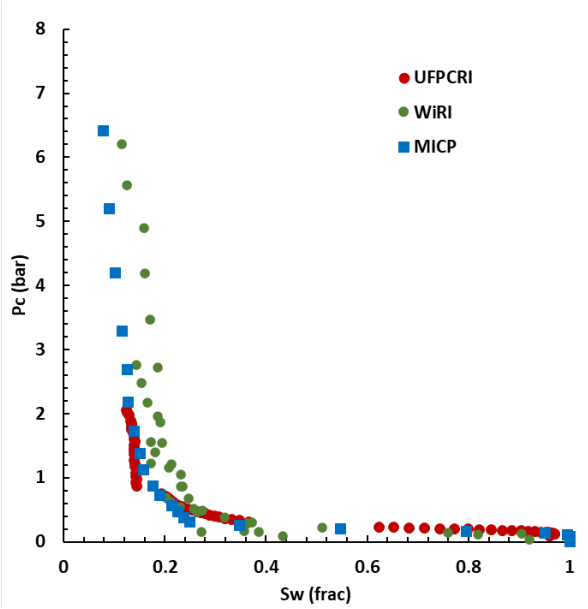

Fig. 10. Pc/Sw curves for sample A3- KgKl = 160 mD: Gas/Water drainage

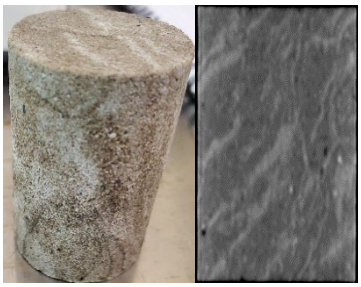

Fig. 11. Photography of the A2 sample at Swi = 17 s.u. on the left – A2 plug CT-scan on the right

Fig. 10 shows a strong disagreement for the n exponent. The Pc/Sw curves from UFPCRI and MICP are superposed while WiRI overestimate Swi.

Fig. 11 left shows the A2 sample in its Swi state. Homogeneity of this sample is clearly questionable and further investigation about its homogeneity could be done from CT scan and an estimation of the coefficient of permeability variation as proposed by Maas *et.al. in* [20] and [21]. Here the lightest parts in the photography are the driest (the most desaturated) while the darkest contains more water. Using a centrifuge, a longitudinal distribution of saturation is expected, whereas here, a radial distribution is (even visually) detected. Since resistivity measurements are acquired with radial electrodes, WiRI process is highly impacted by this effect.

The UFPCRI method is very robust concerning the Pc/Sw curve because Pc is calculated [10] and saturation is measured with NMR (1 measurement each mm). Concerning resistivity and saturation, even with radial electrodes, the UFPCRI resistivity is directly linked to a measured saturation.

Effect of non-Archie behaviour:

Table 5. n exponent and Swi for sample A2 obtained with PP and WiRI

Sample	n exponent	Swi (frac)
A2	PP: 1.60 WiRI: 1.90	PP: 0.09 WiRI: 0.10 (MICP): 0.13

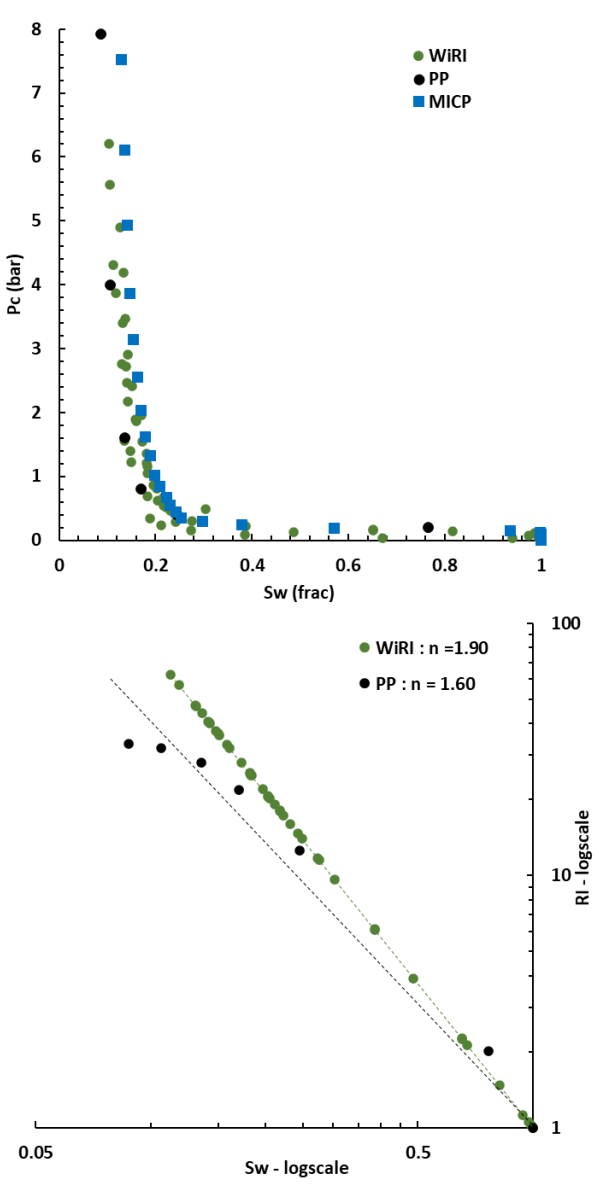

Fig. 12. Pc/Sw curves and log RI/log Sw curves obtained on PP and WiRI for sample A2 – KgKl = 90 mD

In Fig. 12, for sample A3 the n exponent clearly disagrees (n = 1.9 for WiRI and n = 1.6 for PP) while the pc curves do not show different behaviour.

The curvature of logRI/logSw shown in PP is completely missed by WiRI. It is the consequence of Archie's inversion, leading to a straight line in the logRI/logSw plot. Han *et.al.*[22] have shown that a negative deviation at low saturation range could appear due to a water film conduction. With the assumption of validity of Archie's law, WiRI is not able to reconstruct a curvature neither due to a water film nor to any other factor. For the PP experiment, the choice is given to the engineer to choose the model that best describes the observed results. In that case, a Waxman-Smits model (1968) [23], [24], could be a good choice due to the presence of 6% of clays (mainly composed by illite and glauconite) in this sample.

CONCLUSION

In conclusion, simulations have been done with two purposes:

- Investigate and determine which parameter (RI Sw) influences the most the determination of Archie's n exponent. The PP technique is the most impacted, then WIRI and last UFPCRI. The 3 methods are more sensitive to an error on produced volume than to an error on resistivity.

- Investigate the "robustness" of 3 methods to different samples (in terms of K, Pc) when measurements suffer from an error. In the PP technique, investigation of "high" permeabilities would generally lead to a tighter P5-P95 confidence interval due to higher produced volume. UFPCRI is robust to changes in sample characteristics. WiRI shows a small deviation due to its resolution combined with optimization process. When permeability increases, the convexity of the saturation profiles increases. The more convex, the more n is impacted.

While results of simulations only could lead to prefer the use UFPCRI for its major advantages (robustness over different samples, narrower error bars around the n exponent and the possibility to detect heterogeneity during the experiment [8]), the two other methods have shown to be also very robust during experiments. Introduction of handling errors, operators experience and other factors than only measurement errors have, nevertheless, led to determine n exponent with a maximum difference of 0.1 with the 3 methods on homogenous samples. Pc curves shows the same behaviour and at the same pressures, saturations are in a confidence interval of ± 5 s.u.

Simulations have shown that, among the 3 methods, the PP is the most impacted by errors. However, it allows determining RI/Sw relationship under every circumstance (such as a "non-Archie" behaviour).

Last, WiRI simulations have shown a deviation of the n exponent depending on the sample characteristics (K, Pc). Two experiments have shown the limitations of the method and why it should be used only under the assumptions (homogeneity and Archie behaviour) described in [9] otherwise the possibility to estimate a wrong n exponent is quasi-certain. Furthermore, homogeneity needs to be assessed quantitatively through X-CT in order to use a cut off value [21] and also to direct studies towards the most appropriate method. However, the WiRI experiment is an asset of real interest when it comes to quickly determine Pc/Sw and n exponent on homogeneous samples. Fig. 13 is a summary of durations of each experiment for each sample of this study. The graph clearly shows that WiRI proved to be much shorter to determine Pc/Sw and n exponent for all samples.

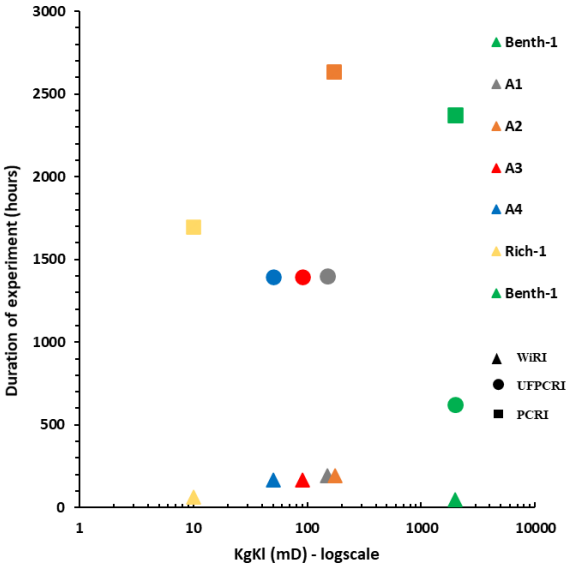

Fig. 13. Total duration of experiment versus Klinkenberg corrected gas permeability for each sample presented in this paper. WiRI is the shortest experiment (10 days maximum for the presented samples). UFPCRI duration is about 2 months and PP about 4 months. For the Richemont sample Swi was not reached neither for PP nor for WiRI

The authors thank Cyril Caubit and Pierre-Edouard Schreiber for their involvement in the management and the development of this project.

REFERENCES

[1] C. McPhee, J. Reed, I. Zubizarreta, "Core analysis: a best practice guide", Elsevier, 2015.

[2] D. Tiab, E.C. Donaldson, "Petrophysics: theory and practice of measuring reservoir rock and fluid transport properties", Gulf professional publishing, 2015.

[3] G.E. Archie, "The Electrical Resistivity Log as an Aid in Determining Some Reservoir Characteristics." Trans 146: 54–62, (1942)

[4] J.A de Waal, R.M.M Smits J.D. de Graaf, B.A. Schipper, “Measurement and evaluation of resistivity index curves”. SPWLA Thirtieth Annual Logging Symposim, June 11-14, 1989

[5] M. Fleury, "FRIM: A Fast Resistivity Index Measurement Method," in SCA, paper 29, (1998)

[6] M. Fleury, “Advances in resistivity measurements using the FRIM method at reservoir conditions. Application to carbonates” in SCA, paper 31, (2003)

[7] N. Bona, E. Rossi, B. Bam, "Ultrafast Determination of Archie and Indonesia m&n Exponents for Electric log Interpretation: a Tight Gas Example", IPTC-17446-MS, (2014)

[8] P. Faurissoux, A. Colombain, G. Pujol, O. Fraute, B. Nicot, “Ultra Fast Capillary Pressure and Resistivity Index measurements (UFPCRI) combining Centrifugation, NMR Imaging, and resistivity Profiling” in SCA, paper 2, (2017)

[9] Q. Danielczick, P. Faurissoux, B. Nicot, ‘Wireless Acquisition for Resistivity Index in Centrifuge – WiRI: A new method to estimate Archie’s law Parameters”, in SCA, paper 18, (2021)

[10] D. Green, J. Dick, J. Gardner, B. Balcom, B. Zhou, "Comparison Study of Capillary Pressure Curves Obtained Using Traditional Centrifuge and Magnetic Resonance Imaging Techniques", in SCA, paper 30, (2007)

[11] D. Green, J. McAloon, P. Cano-Barrita, J. Burger, B. Balcom, "Oil/Water Imbibition and Drainage Capillary Pressure Determined by MRI on a Wide Sampling of Rocks", in SCA, paper 1, (2008)

[12] W. Krauth, “Introduction to Monte Carlo algorithms” summer school in Beg-Rohu (France) and Budapest 1996, 2006. cel-00092936

[13] https://scores-panterra.nl/

[14] J.G. Maas, B. Flemisch, A. Hebing, “Open Source Simulator DuMu^{X}Available for SCAL Data Interpretation”, in SCA, Paper 8, (2011)

[15] http://www.cydarex.fr/

[16] R. Lenormand, K. Lorentzen, J.G. Maas, D. Ruth, “Comparison of Four Numerical Simulators for SCAL Experiments” in SCA, paper 6, (2016)

[17] CYDAR-SCAL User Manual – April 2021– p.43 on: http://cydarex.fr/files/CYDAR_SCAL.pdf

[18] “Randn function” https://fr.mathworks.com/help/matlab/ref/randn.html

[19] F. Pairoys, “Rock Electrical Properties from Porous Plate and Resistivity Experiments: Tips to Maximize Data Quality”, in SCA, Paper 38, (2018)

[20] J.G. Maas, A. Hebing, “Quantitative X-ray CT for SCAL Plug Homegenity Assessment”, in SCA, Paper 4, (2013)

[21] J.G. Maas, N. Springer, A. Hebing, “Defining a sample heterogeneity cut-off value to obtain representative Special Core Analysis (SCAL) measurements”, in SCA, paper 24, (2019)

[22] M. Han, M. Fleury, P. Levitz, “Effect of the pore structure on Resistivity Index curves” in SCA, paper 34 (2007)

[23] M.H. Waxman, L. J. M. Smits, “Electrical Conductivities in Oil-Bearing Shaly Sands”, Society of Petroleum Engineers Journal, SPE-1863-A, June (1968)

[24] M.H. Waxman, E.C. Thomas, “Electrical Conductivities in Shaly Sands-I. The Relation Between Hydrocarbon Saturation and Resistivity Index; II. The Temperature Coefficient of Electrical Conductivity”, Journal of Petroleum Technology, SPE-4094-PA, February. (1974)